A Robust Local Spectral Descriptor for Matching Non-Rigid Shapes with Incompatible Shape Structures

Yiqun Wang[1,2], Jianwei Guo[1]*, Dong-Ming Yan[1]*, Kai Wang[2], Xiaopeng Zhang[1]

[1]NLPR, Institute of Automation, Chinese Academy of Sciences
[2]University of Chinese Academy of Sciences
[2]University Grenoble Alpes, CNRS, Grenoble INP, GIPSAlab

This supplemental material provides extra proof of the proposed LPS feature and more results for LPS and our learned descriptor. In the first section, we provide proof of scale and rotation invariance of LPS feature. In the second section, more comparison results are presented to supplement the paper. Our LPS feature and newly-learned descriptor are tested between different vertex numbers. In addition, we also test our approach on another dataset, SCAPE, to show we have good generalization ability.

1. Invariant properties of scaling and rotation

Review Equation (4) in the paper, we know that the eigenvectors are orthonormal in terms of $\mathbf{A}$-inner product. So there is an implicit constraint here, which is

$$\langle \mathbf{\Phi}_i, \mathbf{\Phi}_j \rangle_A = \mathbf{\Phi}_i^T A \mathbf{\Phi}_j = \delta_{ij} \tag{S1}$$

Given a surface $\mathcal{S}$ and $\mathcal{S}' = \kappa S$ which is scaled by a factor κ. The new matrix $\mathbf{A}' = \kappa^2 \mathbf{A}$ which represents the area and $\mathbf{f}' = \kappa \mathbf{f}$ which represents the coordinate. From Equation (S1), if $i = j$, we can deduce $\mathbf{\Phi}'_j = \frac{1}{\kappa} \mathbf{\Phi}_j$. Recall the Equation (4), because angle does not change due to scale changes, so $\mathbf{T}$ does not change due to scale changes. Therefore, $\lambda' = \frac{1}{\kappa^2} \lambda$. From the Equation (7), we know $\sigma_j = \mathbf{f}^T \mathbf{A} \mathbf{\Phi}_j$, so $\sigma'_j = \kappa^2 \sigma_j$.

Review the original energy of different frequency bands $\widetilde{E}_j = \lambda_j \sum_{i=1}^{d} \sigma_{ij}^2$, the scaled energy $\widetilde{E}'_j = \kappa^2 \widetilde{E}_j$. From this we can see that if the energy is multiplied by λ_j, then the energy is independent of the scale change. We perform the square root operation of the energy multiplied by λ_j, so the final energy on each band is expressed as follows.

$$\widetilde{E}_j = \lambda_j \sqrt{\sum_{i=1}^{3} \sigma_{ij}^2} \tag{S2}$$

*Corresponding authors: jianwei.guo@nlpr.ia.ac.cn, yandongming@gmail.com

For rotation invariance, if the model is rotated, then $\mathbf{F}' = \mathbf{FR}$. Discrete energy $\widetilde{E}'_j$ can be expressed as

$$\widetilde{E}'_j = \lambda_j \sqrt{\mathbf{\Phi}_j^T \mathbf{A}^T \mathbf{F}' \mathbf{F}'^T \mathbf{A} \mathbf{\Phi}_j} \tag{S3}$$

$$= \lambda_j \sqrt{\mathbf{\Phi}_j^T \mathbf{A}^T \mathbf{FR} \mathbf{R}^T \mathbf{F}^T \mathbf{A} \mathbf{\Phi}_j}. \tag{S4}$$

Because the rotation matrix has property $\mathbf{RR}^T = \mathbf{I}$, and then

$$\widetilde{E}'_j = \lambda_j \sqrt{\mathbf{\Phi}_j^T \mathbf{A}^T \mathbf{FF}^T \mathbf{A} \mathbf{\Phi}_j} = \widetilde{E}_j. \tag{S5}$$

Therefore, rotation also has no effect on our proposed LPS features.

2. More results

We present more comparisons of different local descriptors with different resolutions. We perform different tests on other incompatible data. Three learned descriptors (OSD [5], CGF32 [3] and LDGI [8]) and four hand-crafted alternatives (SI [2], SHOT [7], RoPS [1] and HKS [6]) are chosen for comparison.

Fig. 1 shows the matching results on SCAPE dataset, in which 'OURS SCAPE' means shape matching on SCAPE using our learned descriptors and 'OUR-LPS SCAPE' means shape matching on SCAPE using our unlearned LPS features. It should be noted that all of learned descriptors are trained on FAUST and tested on SCAPE. Fig. 2 and Fig. 3 show the matching results between multi-resolution data instead of original training data, in which 'OURS mK-nK' means shape matching between two different resolutions of shapes with mK and nK points using our learned descriptors and 'OUR-LPS mK-nK' means shape matching between two different resolutions of shapes with mK and nK points using our unlearned LPS features. Fig. 4 and Fig. 5 show the other two comparison results to supplement the body of the text, in which 'OURS Ori-nK' means shape matching between original shape and high-resolution shape with nK points.

Figures 1 to 5 show the performance on all the descriptors using the standard *cumulative match characteristic* (CMC) and *Princeton protocol* (PP) [4]. As can be observed, the descriptors we have learned show good generalization capabilities on SCAPE dataset and different resolutions. In addition, our approach achieves the best results compared to other local descriptors.
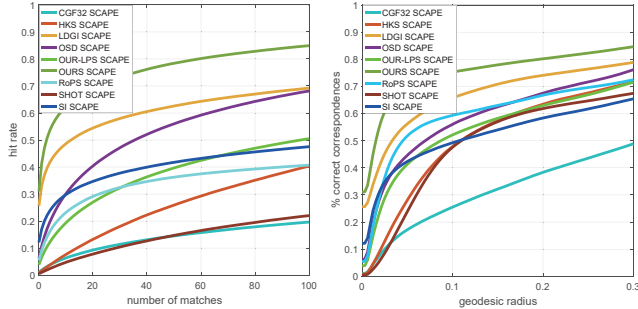

Figure 1. Performances of different descriptors for dense matching on SCAPE model library. Left: CMC curve. Right: correspondence quality of geodesic error.
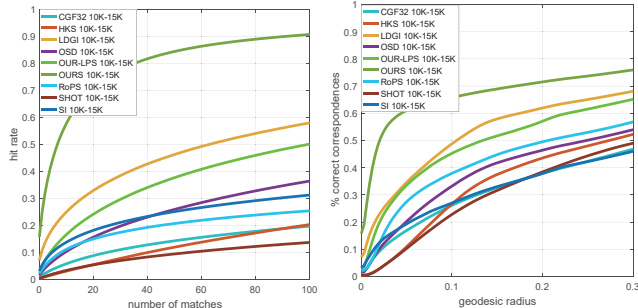

Figure 2. Performances of different descriptors for dense matching between resolution 10K and 15K. Left: CMC curve. Right: correspondence quality of geodesic error.
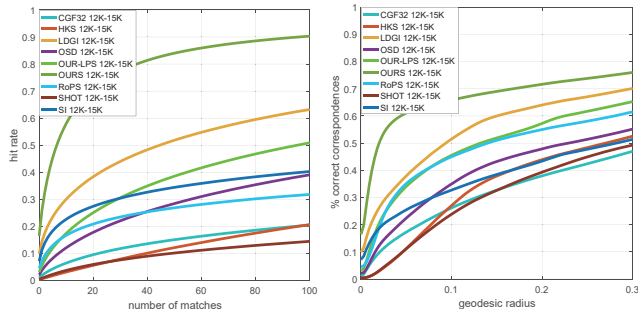

Figure 3. Performances of different descriptors for dense matching between resolution 12K and 15K. Left: CMC curve. Right: correspondence quality of geodesic error.

Affect of geodesic diameter. We perform a new test using different sizes of the geodesic disk. We choose six geodesic radii, which are $3.3\rho_0$, $4.5\rho_0$, $6.5\rho_0$, $9.0\rho_0$, $10.0\rho_0$ and
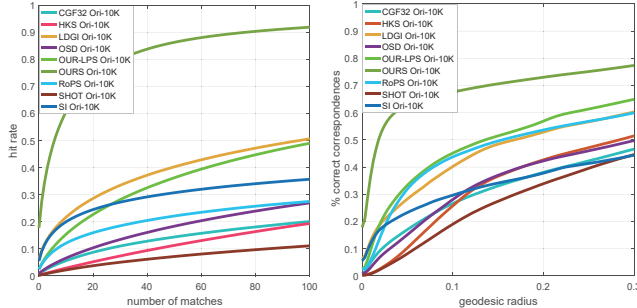

Figure 4. Performances of different descriptors for dense matching between resolution 6890 and 10K. Left: CMC curve. Right: correspondence quality of geodesic error.
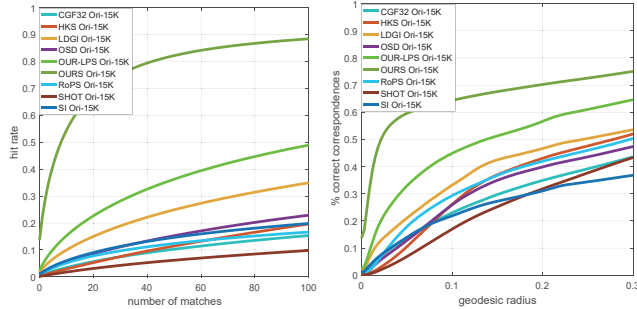

Figure 5. Performances of different descriptors for dense matching between resolution 6890 and 15K. Left: CMC curve. Right: correspondence quality of geodesic error.
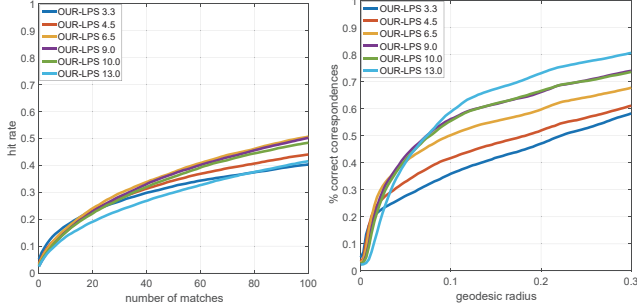

Figure 6. LPS testing results using different geodesic diameters.

$13.0\rho_0$. As the radius of the disk expands, the accuracy of CMC has an extreme value when ratio is 6.5, and then decreases, but PP increases with the increasing of geodesic radius (see Fig. 6). In all of our experiments, we balance both factors simultaneously and choose 6.5 & $9.0\rho_0$ to construct our LPS feature.

References

[1] Y. Guo, F. Sohel, M. Bennamoun, M. Lu, and J. Wan. Rotational projection statistics for 3d local surface description and object recognition. *Int. Journal of Computer Vision*, 105(1):63–86, 2013.

[2] A. E. Johnson and M. Hebert. Using spin images for efficient object recognition in cluttered 3d scenes. *IEEE Trans. on Pat-*

tern Analysis and Machine Intelligence, 21(5):433–449, May 1999.

[3] M. Khoury, Q.-Y. Zhou, and V. Koltun. Learning compact geometric features. In *IEEE Computer Vision and Pattern Recognition (CVPR)*, pages 153–61, 2017.

[4] V. G. Kim, Y. Lipman, and T. Funkhouser. Blended intrinsic maps. *ACM Trans. on Graphics*, 30(4):79:1–79:12, July 2011.

[5] R. Litman and A. M. Bronstein. Learning spectral descriptors for deformable shape correspondence. *IEEE Trans. on Pattern Analysis and Machine Intelligence*, 36(1):171–180, 2014.

[6] J. Sun, M. Ovsjanikov, and L. J. Guibas. A concise and provably informative multi-scale signature based on heat diffusion. *Computer Graphics Forum*, 28(5):1383–1392, 2010.

[7] F. Tombari, S. Salti, and L. Di Stefano. Unique signatures of histograms for local surface description. In *European Conference on Computer Vision (ECCV)*, pages 356–369. Springer, 2010.

[8] H. Wang, J. Guo, D.-M. Yan, W. Quan, and X. Zhang. Learning 3d keypoint descriptors for non-rigid shape matching. In *European Conference on Computer Vision (ECCV)*, pages 3–20. Springer, 2018.